ISSN 1392–1320 MATERIALS SCIENCE (MEDŽIAGOTYRA). Vol. 19, No. 3. 2013

Effect of Heat Treatments on the Microstructure, Hardness and Corrosion Behavior of Nondendritic AlSi9Cu3(Fe) Cast Alloy

Nacer ZAZI *

University Mouloud Mammeri of Tizi-Ouzou, Faculty of Construction Engineering, Department of Mechanical Engineering (LMSE), B.P.17 RP Tizi-Ouzou, Algeria

crossref http://dx.doi.org/10.5755/j01.ms.19.3.1397

Received 22 March 2012; accepted 19 March 2013

In this paper we studied the influence of heat treatments on properties of AlSi9Cu3(Fe) nondendritic cast alloy. Solution heat treatment, six hours at 520 °C, while making the grains more spherical modifies corrosion morphology into intergranular corrosion and corrosion surrounding spherical particles in 3 % NaCl solution. Past solution treatment, quenching at 520 °C after one hour with two weeks of natural aging transform the shape of grains into equiaxes form. Two weeks of natural aging and 30 minutes of aging at 150, 200, 250 °C after solution treatment and quenching give birth to the "Chinese script" form of the $Al_{15}(MnFe)_3Si$ intermetallic particles. The prolongation of the duration period of aging to one hour at 200 °C is sufficient to transform the morphology of corrosion into located corrosion by pitting, and a longer aging cancels the "Chinese script" form.

Keywords: AlSi9Cu3 alloy, intermetallic phases, heat treatment, mechanical properties, corrosion.

1. INTRODUCTION

These last years the development of the automotive industry is based on light materials, allowing an economy in the fuel consumption.

The aluminum alloys represent a significant category of materials due to their high and extended technological value, particularly in aerospace industries.

The use of alloys of the system of AlSi9CuX has become increasingly significant these last years, mainly in the car industry which employs recycled aluminum, in the form of various frames of engine, pistons, cylinder heads, exchangers of heat, air-conditioners, wheels, shock absorbers, floor of loads and components of suspension. This is due to their high strength at ambient as well as at high temperature [1, 2]. The high percentage of silicon of these alloys confers a better fluidity and a higher flow [3]. Aluminum alloys replace grey cast iron in many demanding applications [2]. In the structure of alloy of foundry AlSi9Cu3, evolution of primary aluminum phase and intermetallics phases involve a change of the mechanical and electrochemical properties. This means that there is a relation between the composition, the form and the dimension of the primary aluminum matrix and the intermetallics phases, hence between mechanical and electrochemical properties.

The cast alloy of AlSi9Cu3, is characterized by a primary aluminum matrix, of dendritic structure of the solid solution α, by a discontinuous phase α+β-Silicon forming the eutectic grains and many other intermetallic particles [4 – 6]. L. A. Dobrzański et al. studied cast alloys AlSi9CuX and showed that the intermetallic phases β-Silicon form large flakes, needles and fibrous precipitations. They quoted five phases and four reactions of solidification. Mechanical properties AlSi9Cu3 alloy are controlled by the reinforcement of the primary aluminum matrix by the other and the dispersion of the β-Silicon phases: these can be improved by heat treatment [3]. In commercial aluminum-silicon cast alloys, iron form fragile intermetallic particles. The nondendritic structure of semi-solid metals, with globular grains, obtained by starting from semi-solid aluminum alloy muds to have mechanical properties larger than those of the materials obtained by traditional casting, which is of a great economic interest during the recycling of these alloys; the explanation of the conditions and the mechanism of the formation of these structures has a great scientific interest [7].

Spacings between the axes of dendrites models of segregation, nature, size, distribution and morphology of the intermetallic particles and porosity, all affect the final mechanical and electrochemical properties. Porosity also has a noxious effect on the workability [8].

In Al-Si-Cu alloys, solution treatment at relatively high temperatures is applied to homogenize the alloy elements in the primary solution, dissolve the intermetallic particles with easy dissolution such as, ß-Mg_2Si, ϴ-Al_2Cu and causes the eutectic spheroidization of the particles containing silicon which have a great impact on the mechanical properties of alloy. On the other hand, this treatment does not dissolve the intermetallic particles with hard dissolution such as π-$Al_8Mg_3FeSi_6$, Q-$Al_5Cu_2Mg_8Si_6$, and α-$Al_{15}(Fe,Mn)_3Si_2$. A prolongation of the duration period at temperature of solution treatments fragment plates ß-Al_5FeSi phases. A long time of maintenance at this temperature undergoes progressive dissolution of ß-Al_5FeSi phases [9, 10].

Quenching, at room temperature, is used to obtain a solution supersaturated in solute atoms vacancies and gaps in the primary phase. Firstly, the quantity of silicon in excess in the primary solid solution is reduced by diffusion of the silicon atoms into eutectic silicon particles. Secondly, the phase of Mg_2Si nucleates on the eutectic

* Corresponding author. Tel.:+213-551577720, fax: +213-26215674.
E-mail address: *zazinacer@yahoo.fr* (N Zazi)

Table 1. Chemical composition of AlSi9Cu3 (Fe) cast alloy

Element	Al	Si	Cu	Mg	Mn	Ni	Fe	Zn	Sn	Pb
wt.%	Bal.	9.42	3.40	0.18	0.54	0 .72	1.20	1.10	0.10	0.34

particles containing silicon, reduces the concentration of magnesium in the primary solid solution. Finally, the presence of the eutectic silicon particles increases the density of dislocation, due to the difference of thermal expansion between silicon and aluminum atoms, which provides nucleation sites of precipitates [9, 11]. The quenching retains the solute atoms and some gaps in the lattice structure of a supersaturated solid solution, which are produced during solution heat treatment by rapidly cooling the specimens at a lower temperature, resulting in hardening by precipitation [3]. Age hardening, natural or artificial aging, produces a small precipitates particles uniformly distributed and dispersed. During the last series of changes in microstructure we obtain high mechanical strength [3, 9, 11, 12].

For different aluminum alloys, the MgSi particles activate anodic dissolution of Mg within first seconds of immersion in aggressive chlorides containing solution [13]. According to S. Bjørn Tenam et al. [14], the particles comprising magnesium in their composition, such as the particles MgSi and AlCuMgSi are less noble than the aluminum matrix. When Mg of π-$Al_8Mg_3FeSi_6$ and Q-$Al_5Cu_2Mg_8Si_6$ is dissolved, the particles become nobler and do not comprise magnesium in their composition. The AlMnFeCuSi particles are nobler than the aluminum matrix [14].

Al_2Cu is relatively cathodic compared with the α-Al [15], α-Al_{15} $(Fe,Mn)_3Si_2$ phases is nobler than matrix [16]. It has been established that the distribution of magnesium and silicon becomes homogeneous in less than one hour of solution treatment. It has also been reported that heat treatment solution changes the morphology of eutectic silicon from a polyhedral into globular structure [17]. The quenching process produces Mg, Cu and Si supersaturated solid solution, but aging result is the hardening by precipitation [3]. This means the corrosion of alloy AlSi9Cu3 (Fe) is influenced by undergone heat treatments.

The aim of this work is to show the existence of hypoeutectic aluminum cast alloy AlSi9Cu3 (Fe) with nondendritic structure, and study the effect of the heat treatments (solution treatment, natural ageing and artificial ageing) on hardness and on corrosion behavior in 3 % NaCl solution of this alloy.

2. EXPERIMENTAL TECHNIQUES AND METHODS

The analyzed material is a hypoeutectic aluminum cast alloy AlSi9Cu3 (Fe). The chemical composition of the alloy is shown in Table 1. The experimental cast simples are prepared from an ingot of industrial origin.

The heat treatments were carried out in an electric furnace. Two series of twelve samples have been performed during six hours and cooled in the furnace by annealing at 520 °C. Eleven of these samples undergo a heating during one hour at 520 °C, followed by cooling in cold water. One of the samples was aged two weeks at room temperature 25 °C. Nine samples undergo an artificial aging at different temperatures and time of maintenance (Table 2).

The choice of the heat treatment at 520 °C is due to the fact that eutectic silicon of the dendritic AlSi9Cu3 cast alloy at 505 °C is fragmentized into smaller spherical particles, however 505 °C is not sufficient for spheroidized particles, but they has been observed in partially rounded shape [1, 5, 12]. Optimal solution treatment temperature is at 515 °C, when has eutectic silicon fine, completely rounded shape and bars of eutectic silicon are evident partially [1, 5, 12]. Solution treatment at 525 °C causes perfect spheroidization of eutectic silicon, but after four hours leads to globular silicon particles significant coarsening [1, 5, 12].

The choice of six hours maintenance at 520 °C is due to the fact that after annealing at 515 °C during four hours, which represents a regime where optimal structural factors are achieved even the best mechanical properties were realized, but after eight hours maintenance the value of mechanical properties begins to decrease [1, 5, 12]. Fracture limit increases from 211 MPa in starting stage, to 273 MPa and hardness from 98 HBS to 122 HBS after four hours maintenance time at 515 °C [1, 5, 12]. Prolongation of the maintenance time for six hours allows to obtain the most spherical possible granulometry form of aluminum matrix. If time of maintenance exceeds six hours at 515 °C and 525 °C the silicon particles dimension do not change much [5].

The samples for microscopic analysis of dimensions (30×30×25 mm) were cut out using a mechanical saw and prepared by standard metallographic procedures: grinded, polished with alumina suspensions, cleaned with alcohol then water and cool-dried before each experiment. One series of these samples was etched by reagent constituted of 5 % HF, 9 % HCl, 23 % HNO_3 and 63 % H_2O, the time of etching for each specimen was between 10 s – 15 s. After this, the microstructural details were analyzed using optical microscopy. Other series of samples was prepared for the electrochemical analysis, followed by observation of microstructures corrosion after two weeks of immersion in

Table 2. Temperature and maintenance of aging for the annealed 6 h at 520 °C and quenched after one hour at 520 °C samples of AlSi9Cu3 (Fe) cast alloy

Sample	1	2	3	4	5	6	7	8	9
Temperature of aging (°C)	150	150	150	200	200	200	250	250	250
Maintenance time (min)	30	60	90	30	60	90	30	60	90

3 % sodium chloride solution. The optical microstructures were taken by Carl Zeiss ICM405 microscopy with different magnifications up to 1000×.

Hardness measurements were taken with model Frank Weinheim-Birkrnau type 38500 hardness tester; the HRA scale was chosen for the testing of this specimen: at least five measurements by samples were examined.

The electrochemical measurements have been undertaken with 1-cm^2 samples immerged in a sodium chloride solution (3 % weight) at room temperature. A classic three-electrode method has been used. The reference electrode is silver/silver chloride electrode; the auxiliary electrode is a platinum foil. Rest potential curves has been obtained by means of a radiometer potentiostat (PGP 201) controlled by Voltamaster 4 software.

3. RESULTS AND DISCUSSION

Fig. 1, a, shows the microstructure of the untreated cast alloy AlSi9Cu3 (Fe). We do not observe a dendritic primary phase, but we see grains close to spherical form of an average diameter of 100 μm. The investigated AlSi9CuX hypoeutectic cast alloys series show the formation of aluminum rich phase (α-Al) in dendritic form [1, 6, 12, 18]. Platelets of eutectic silicon (white phases), and Al_2Cu phases in form bulk precipitates (brown particles) in grains boundary. Finer particles eutectic Al+Al_2Cu in the bulk of the grains, and a dark grey of iron-rich intermetallic phases $Al_{15}(MnFe)_3Si$, and ultra fine invariant quaternary eutectic $Al_5Mg_8Cu_2Si_6$. This result is in good agreement with E. Tillová et al, L. A. Dobrzański et al, M. Panušková et al, Z. Li et al, and L. Hurtalová et al [1, 6, 12, 18, 19].

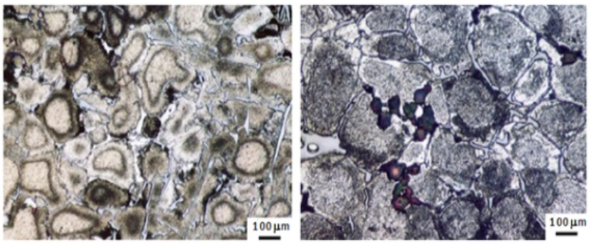

a b

Fig. 1. Microstructure of aluminum cast alloy AlSi9Cu3 (Fe) (a) untreated sample, (b) sample after solution treatment six hour at 520 °C

Six hours solution treatment at 520 °C (Fig. 1, b), causes dissolution of primary phase (α-matrix), iron-rich intermetallic phase ($Al_{15}(MnFe)_3Si$), invariant quaternary eutectic $Al_5Mg_8Cu_2Si_6$, precipitates of Al_2Cu and silicon eutectic, this is in concord with Bäckerud [1, 12]. But during solution treatment at 520 °C and cooling in furnace the primary phase (α-matrix) grows, the size of grains increases and their shape becomes more spherical. The Al_2Cu, silicon eutectic, and iron-rich intermetallic phases ($Al_{15}(MnFe)_3Si$) and $Al_5Mg_8Cu_2Si_6$ phases precipitate and grow around the boundary grains with new form. The eutectic silicon is not any more in the shape of platelets and the brown particles of Al_2Cu are concentrated in some areas of the microstructure (Fig. 1, b).

After six hours solution treatment at 520 °C followed by quenching in cold water after one hour of maintenance at 520 °C and two weeks of ripening (Fig. 2), we obtain a microstructure with finer equiaxes grains. We observe platelets and round eutectic silicon in intergranular regions, grey needles of Al_5FeSi phase and precipitates of $Al_5Mg_8Cu_2Si_6$. This is in good agreement with the work of T. Tański et al. [4]. We also observed Al_2Cu with various shapes; the dominant shape is spherical eutectic which precipitates in the boundary grains and inside the grains in the bulk. Starting from an unstable supersaturated solution, and so the gaps are fixed by quenching, inducing therefore the diffusion of the copper atoms. The $Al_{15}(MnFe)_3Si$ phase with a cubic crystal structure has a compact morphology in the form of "Chinese script" is observed too; this one was described by E. Tillová et al, G. Timelli et al and C. T. Rios et al. [1, 17, 20] (Fig. 2).

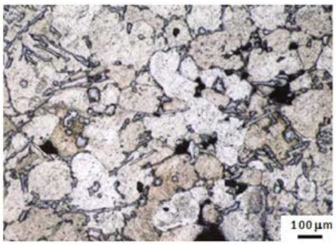

Fig. 2. Microstructure of aluminum cast alloy AlSi9Cu3 (Fe) after solution treatment six hour at 520 °C, quenching at 520 °C after one hour maintenance time and two weeks natural aging

We can see a drop in the value of hardness (4.10 %) of the sample after solution treatment at 520 °C followed by cooling in furnace (Table 3); this is due, in the first instance, to the increase of the grain size, which induces the decrease in the density of the surface defects (grain boundaries). In the second time, when cooled slowly, the Gibbs energy of the precipitation is low and the germination rate is low as well. To ensure proportion of equilibrium precipitates, the rare germs should grow in large precipitates apart from each other at the grain boundaries. It's easy for dislocations to avoid the precipitates. On the other hand, the effect of the partial segmentation of hard particles, Al_5FeSi, $Al_{15}(MnFe)_3Si$, and spheroidization of silicon eutectic on the hardness of the alloy is not apparent because hardness obtained is low.

Increasing of hardness value after solutions treatment followed by quenching and two weeks of ripening at room temperature (Table 3) is due chiefly to a fine precipitation of Al_2Cu particles in the whole volume of the material. The mobile dislocations have evil to cross the precipitates and the alloy becomes therefore harder.

Fig. 3, a, b, c, shows the microstructures of samples which have undergone artificial aging of 30 minutes at temperatures of 150 °C, 200 °C and 250 °C respectively samples (1, 4, 7) (Table 2). In this figure, we notice that the phase $Al_{15}(MnFe)_3Si$ has the form of "Chinese manuscript" and blocky particles, spherical and platelets eutectic silicon at grain boundaries, fine particles Al_2Cu within the grains and intergranular regions in all the volume.

Fig. 4, a, b, c, representing the artificial aging during 90 minutes samples (3, 6, 9) (Table 2) shows the disappearance of the phase $Al_{15}(MnFe)_3Si$ as "Chinese script" but blocky particles do not disappear.

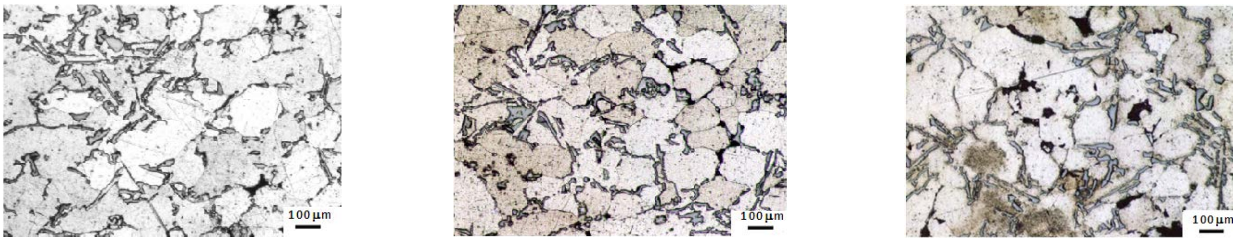

a b c

Fig. 3. Microstructure of aluminum cast alloy AlSi9Cu3 (Fe) having undergone solution treatment six hour at 520 °C, quenching at 520 °C after one hour maintenance time and aged: a – 30 minutes at 150 °C, b – 30 minutes at 200 °C, c – 30 minutes at 250 °C

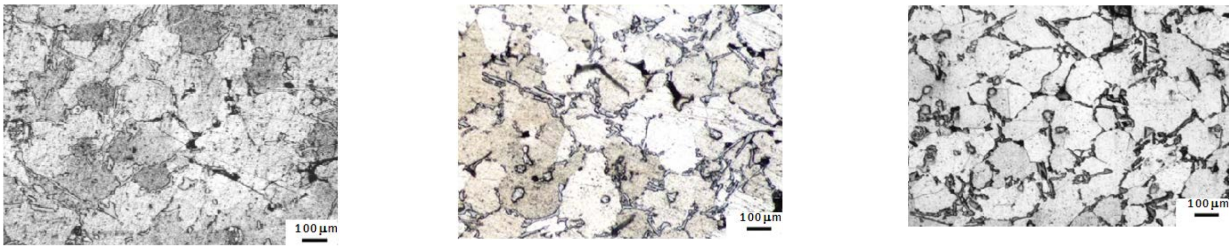

a b c

Fig. 4. Microstructure of aluminum cast alloy AlSi9Cu3 (Fe) having undergone solution treatment six hour at 520 °C, quenching at 520 °C after one hour maintenance time and aged: a – 90 minutes at 150 °C, b – 90 minutes 200 °C, c – 90 minutes 250 °C

After extra time artificial aging at 150 °C up to 90 minutes, we notice finer spheres and platelets eutectic silicon at the grain boundaries, and fine particles of Al_2Cu distributed in all the volume of the material (Fig. 4, a).

After 90 minutes aging at 200 °C, the spheroidized eutectic silicon particles become bigger with a less significant amount (Fig. 4, b). When holding at 250 °C during 90 min, a significant proportion of eutectic silicon spherical coarse is positioned at the grain boundaries of the primary phase. A small part remains in the form of platelets eutectic silicon, a coarsening of Al_2Cu particles by coalescence are distributed throughout the volume of the material (Fig. 4, c).

The increase in hardness after artificial aging of 30 minutes at 150 °C, 200 °C and 250 °C samples (1, 4, 7) (Table 2) is especially due to precipitation of fine particles Al_2Cu in the volume of the material, the formation of spherical eutectic silicon and the hard particle of $Al_{15}(MnFe)_3Si$. The decrease in hardness after 90 min of aging samples (3, 6, 9) (Table 2) is due mainly to the coalescence of precipitates Al_2Cu and disappearance of particles $Al_{15}(MnFe)_3Si$ (Fig. 5).

Fig. 6, a, b, presents the recordings of the potential of corrosion variation, of AlSi9Cu3 (Fe) cast alloy in solution of 3 % of NaCl at room temperature, in function of time. The measurements taken present a high degree of dispersion in the values of the potential of corrosion, both in respect of the initial potential and of its evolution over time. Moreover, it can be observed that the widest differences are in the measurements taken after relatively short exposure of all samples. Sample 1 (Table 2) has nobler corrosion potential. The corrosion potential of all samples decreases in the first days. Recordings of the potential of corrosion at prolonged periods of exposure show that all the curves tend to converge. It follows from this that the difference observed in the potential of corrosion, must be related to differences observed in the number and the dimension of cathodic particles such as, Al_2Cu, α-$Al_{15}(Fe,Mn)_3Si_2$, AlMnFeCuSi and the (π-$Al_8Mg_3FeSi_6$, Q-$Al_5Cu_2Mg_8Si_6$) stripped magnesium by dissolution, existing in the surface of the various studied samples.

The potential value (Fig. 6) shows that the kinetics of corrosion of the various samples is different, this is shown by follow-up of the corrosion potential of over two weeks of immersion in a solution of 3 % NaCl. In conclusion, heat treatments are influential only in the first days after immersion. After this, it is independent of the treatment undergone by material and corresponds only to the process of local passivation which takes place.

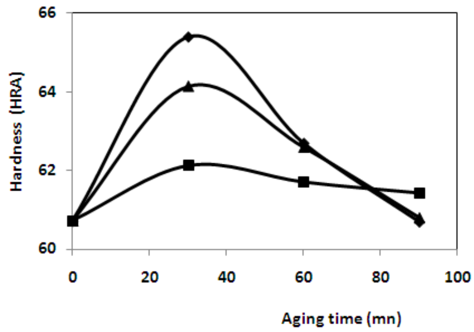

Fig. 5. Hardness (HRA) evolution after solution treatment, quenching then artificial aging of aluminum cast alloy AlSi9Cu3 (Fe): ■ – at 150°C, ▲ – at 200°C, ♦ – at 250°C

Fig. 6, a, indicates that the sample annealed, sample 1 (Table 2) has a nobler and stable corrosion potential value than the other samples. The potential corrosion of sample untreated converges towards the potential corrosion of sample 1. (Fig. 7, a, d) confirms this result because the corrosion morphology of the two samples is similar.

An increase in the aging temperature and prolongation of the aging time, decreases value of corrosion potential of AlSi9Cu3 (Fe) cast alloy, which becomes less noble (Fig. 6, b).

Table 3. Average Rockwell hardness (HRA) values of aluminium cast alloy AlSi9Cu3 (Fe) specimens after various heat treatments

Sample	Untreated	Solution treatment 6 h at 520 °C	Solution treatment followed by Quenching after one hour at 520 °C Cold in Water	Solution treatment followed by Quenching and aged two weeks at 20 °C
Rockwell Hardiesses (HRA)	63.40	60.80	60.70	64.70

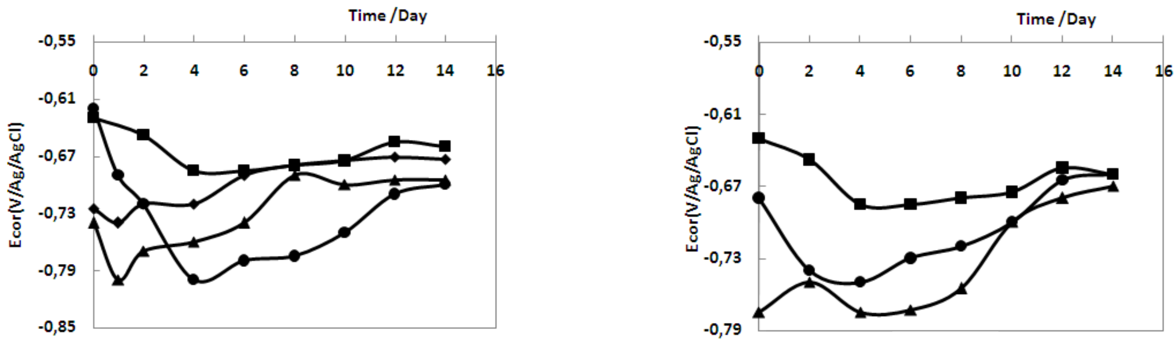

a b

Fig. 6. Corrosion potential of aluminum cast alloy AlSi9Cu3 (Fe): (a) ♦ – untreated sample, ▲ – sample after solution treatment, ● – sample after solution treatment, quenching and natural aging two weeks, ■ – sample after solution treatment, quenching and aged 30 minutes at 150 °C. (b) Samples after solution treatment, quenching and aged: ■ – 30 minutes at 150°C, ● – 90 minutes at 150°C, ▲ – 30 minutes at 250°C

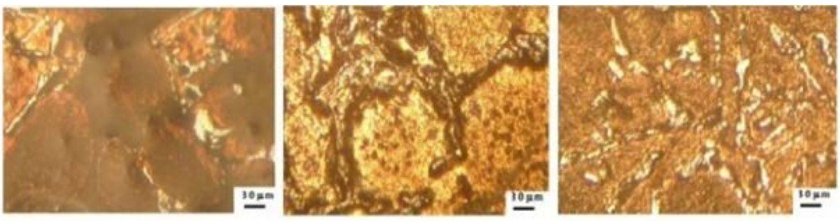

a b c

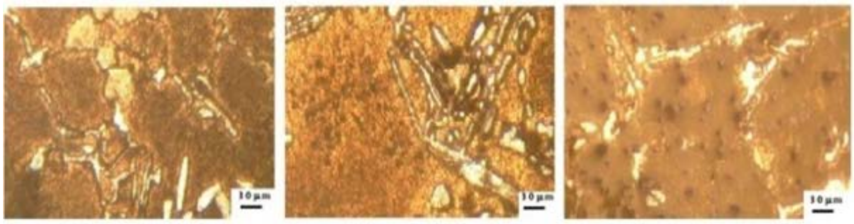

d e f

Fig. 7. Images of samples of aluminum cast alloy AlSi9Cu3 (Fe) after two weeks of immersion in aerated NaCl 3 % solution: a – untreated sample; b – solutions treatments six hour at 520 °C; c – solution treatments, quenching after 1 h maintenance then 2 weeks natural aging; d, e, f – solution treatments, quenching after 1 h maintenance then artificial aging, 30 min at 150 °C, 30 min at 200 °C, 60 min at 200 °C respectively

Corrosion of untreated sample and sample 1 (Table 2) seems to be a generalized corrosion (Fig. 7); this is due to uniform distribution of fine intermetallic particles in surface. Various forms of corrosion morphology are observed in the other samples. The samples having undergone six hours solution treatment at 520 °C, which undergo a quenching after one hour of maintenance at 520 °C, sample 4 (Table 2) corrodes on grain boundary and around the spherical particles precipitates in the bulk of grain (Fig. 7, b, c, e); this is due to the enlargement of the all intermetallic particles.

Sample 5 (Table 2) is corroded by pitting in certain areas (Fig. 7, f); this is especially the result of Al_2Cu precipitates coalescence.

4. CONCLUSIONS

Grains with almost spherical shape and significant values of hardness were observed in the cast alloy AlSi9Cu3 (Fe) untreated of industrial origin.

Ripening and artificial aging with short duration at temperature ranging from 150 °C to 250 °C after six hours solution treatment at 520 °C followed by quenching at 520 °C after one hour of maintenance, give birth to the intermetallic particles $Al_{15}(MnFe)_3Si$ in the form of "Chinese script". But an artificial aging at the same temperatures with longer period of time of maintenance cancels this form.

The significant difference between the hardness's obtained before and after the solution treatment for the

AlSi9Cu3(Fe) cast alloy, results from modification of shape of eutectic silicon and the enlargement of primary phase grains (α-matrix).

The effect of segmentation of hard Al_5FeSi, $Al_{15}(MnFe)_3Si$ on the hardness of the AlSi9Cu3 (Fe) cast alloy is not apparent after six hours of solution treatment at 520 °C.

Heat treatments influence the morphology and the kinetics of corrosion during the first days of immersion in 3 % NaCl solution.

Six hours of solution treatment at 520 °C, followed by quenching at 520 °C after one hour time maintenance, and two weeks of natural aging or 30 minutes of artificial aging at (150 °C, 200 °C) causes the formation of intergranular corrosion and corrosion surrounding spherical intermetallic particles.

Solution treatment followed by quenching, then one hour of artificial aging at 200 °C causes formation of a located corrosion by pitting.

REFERENCES

1. **Tillová, E., Panušková, M.** Effect of Solution Treatment on Intermetallic Phases Morphology in AlSi9Cu3 Cast Alloy *Metalurgija* 47 (3) 2008: pp. 207 – 210.
2. **Kaufman, J. G., Rooy, E. L.** Aluminum Alloy Castings. ASM International, Ohio, 2005: 340 p.
3. **Azmah Hanim, M. A., Chang Chung, S., Khang Chuan, O.** Effect of a Two-step Solution Heat Treatment on the Microstructure and Mechanical Properties of 332 Aluminuim Silicon Cast Alloy *Materials and Design* 32 (4) 2011: pp. 2334 – 2338. http://dx.doi.org/10.1016/j.matdes.2010.12.040
4. **Tański, T., Dobrzański, L. A.**, **Maniara, R.** Microstructures of Mg-Al-Zn and Al-Si-Cu Cast Alloys *Journal of Achievements in Materials and Manufacturing Engineering* 38 (1) 2010: pp. 64 – 71.
5. **Skočovský, P., Tillová, E., Belan, J.** Influence of Technological Factors on Eutectic Silicon Morphology in Al-Si Alloys *Archives of Foundry Engineering* 9 (2) 2009: pp. 169 – 172.
6. **Dobrzański, L. A., Maniara, R., Krupiński, M., Sokolowski, J. H.** Microstructure and Mechanical Properties of AC AlSi9CuX Alloys *Journal of Achievements in Materials and Manufacturing Engineering* 24 (2) 2007: pp. 51 – 54.
7. **Guo, Hong Min., Liu, Xu Bo., Yang, Xiang Jie., Zhang, Ai Sheng., Liu, Yong.** Microstructure Evolution Behavior of AlSi9Cu3 Alloy during Rheocasting *Transactions of Nonferrous Metals Society of China* 20 (9) 2010: pp. 815 – 820. http://dx.doi.org/10.1016/S1003-6326(10)60587-0
8. **Ferreiraa, I. L., Lins, J. F. C., Moutinho, D. J., Gomes, L. G., Garcia, A.** Numerical and Experimental Investigation of Microporosity Formation in a Ternary Al-Cu-Si Alloy *Journal of Alloys Compounds* 503 (1) 2010: pp. 31 – 39. http://dx.doi.org/10.1016/j.jallcom.2010.04.244
9. **Sjölander, E., Seifeddine, S.** The Heat Treatment of Al-Si-Cu-Mg Casting Alloys *Journal of Materials Processing Technology* 210 (10) 2010: pp. 1249 – 1259. http://dx.doi.org/10.1016/j.jmatprotec.2010.03.020
10. **Dinnis, C. M., Taylor, J. A., Dahle, A. K.** Interactions between Iron, Manganese, and the Al-Si Eutectic in Hypoeutectic Al-Si Alloys *Metallurgical and Materials Transactions A* 37A (11) 2006: pp. 3283 – 3291.
11. **Petrič, M., Medved, J., Mrvar, P.** Effect of Grain Refinement and Modification of Eutectic Phase on Shrinkage of AlSi9Cu3 Alloy *Metalurgija* 50 (2) 2011: pp. 127 – 131.
12. **Panušková, M., Tillová, E., Chalupová, M.** Relation between Mechanical Properties and Microstructure *Strength of Materials* 40 (1) 2008: pp. 98– 101.
13. **Ackermann, F., Suter, T., Ugowitzer, P. J., Afseth, A., Schmutz, P.** The Influence of MgSi Particle Reactivity and Dissolution Processes on Corrosion in Al-Mg-Si Alloys *Electrochimica Acta* 54 (2) 2008: pp. 844 – 855. http://dx.doi.org/10.1016/j.electacta.2008.05.078
14. **Tenam, B. S., Svenningsen, G., Mårdalen, J.** Relations between Sample Preparation and SKPFM Volta Potential Maps on an EN AW-6005 Aluminium Alloy *Corrosion Sciences* 47 (6) 2005: pp.1506 – 1519. http://dx.doi.org/10.1016/j.corsci.2004.07.029
15. **Lu, R., Fereirra, M. G. S., Alemeida, A., Vilar, R., Watkins, K. G., McMahon, M. A, Steen, W. M.** Localized Corrosion of Laser Melted 2024-351 Aluminium Alloy *Surface and Coatings Technology* 81 (2– 3) 1996: pp. 290 – 296.
16. **Yasakau, K. A., Zheludkevich, M. L., Lamaka, S. V., Ferriera, M. G. S.** Role of Intermétallic Phases in Localized Corrosion of AA5083 *Electrochimica Acta* 52 (27) 2007: pp. 7651 – 7659. http://dx.doi.org/10.1016/j.electacta.2006.12.072
17. **Timelli, G., Bonollo, F.** The Influence of Cr Content on the Microstructure and Mechanical Properties of AlSi9Cu3(Fe) Die-casting Alloys *Materials Science and Engineering A* 528 (1) 2010: pp. 273 – 282. http://dx.doi.org/10.1016/j.msea.2010.08.079
18. **Li, Z., Samuel, A. M., Samuel, F. H., Ravindran, C., Valtierra, S., Doty, H. W.** Parameters Controlling the Performance of AA319-type Alloys. Part I. Tensile Properties *Materials Science and Engineering A* 367 (1 – 2) 2004: pp.96 – 110.
19. **Hurtalová, L., Tillová, E., Chalupová, M.** Cu-rich Intermetallic Phases in Recycled AlSi9Cu3 Cast Alloy – a Comparison Between Aging Behavior in T4 and T6 Treatments *Perner's Contact* 6 (2) 2011: pp. 72 – 80.
20. **Rios, C. T., Caram, R.** Intermetallic Compounds in the Al-Si-Cu system *Acta Mikroskopica* 12 (1) 2003: pp 77 – 81.